

# Adaptive method for assessing information reliability under uncertainty for 5G and IoT systems

Serhii Zaitsev<sup>1,2</sup>, Vladyslav Vasylenko<sup>2</sup>, Vasyl Trysnyuk<sup>2</sup>, Taras Trysnyuk<sup>2</sup>

*1 Kielce University of Technology (Politechnika Świętokrzyska), Kielce, Poland, aleja Tysiąclecia Państwa Polskiego 17B, tel. +48-606-559-002*

*2 Institute of Telecommunications and the Global Information Space of the National Academy of Sciences of Ukraine, Chokolivsky Boulevard 13, Kyiv, 02000, Ukraine*

## Abstract

The article proposes a method for assessing the reliability of information in high-speed transmission of information over radio channels in conditions of increased noise. The method is based on the calculation of the decoding inaccuracy index (error rate) by the maximum a posteriori probability in systems with multi-parameter adaptation in terms of parameters of error-correcting codes, in particular, turbo codes and codes with low parity check (Low-Density Parity-Check Codes - LDPC). The method provides an increase in the accuracy of decision-making when assessing the reliability of information with an adaptive change in the encoding rate and polynomials of component encoders/decoders under conditions of uncertainty caused by increased data noise.

## Keywords

Turbo codes, LDPC-codes, uncertainty, reliability of information, modeling.

## 1. Introduction

Currently, there is a trend of rapid development of wireless technologies.

In recent years, the fifth generation mobile communication technology 5G has been widely developed and implemented [1, 2], which has several advantages compared to 4G, namely:

- low signal delay;
- increased bandwidth;
- increased user mobility;
- higher data transfer speed (peak speed of 20 Gbit/s);
- increased transmission speed.

A number of these advantages allow us to continue development in the following areas[3,4]:

- Internet of Things (IoT) – smart house, smart city, etc.;
- unmanned transport;
- cloud technologies (data storage, cloud computing);
- health care;
- virtual reality.

Proceedings ITTAP'2023: 3rd International Workshop on Information Technologies: Theoretical and Applied Problems, November 22–24, 2023, Ternopil, Ukraine, Opole, Poland

EMAIL: szaitsev@tu.kielce.pl (A.1); vladvasilenko9@gmail.com(B.1); tryznyuk@ukr.net(B.2); taras24t@gmail.com(B.3)

ORCID: 0000-0001-6643-917X (A.1); 0000-0001-8156-1894 (B.1); 0000-0001-9920-4879(B.2); 0000-0002-3672-8242(B.3)



© 2020 Copyright for this paper by its authors.  
Use permitted under Creative Commons License Attribution 4.0 International (CC BY 4.0).  
CEUR Workshop Proceedings (CEUR-WS.org)

In this regard, one of the main tasks is to evaluate the channel, increase the reliability of information transmission and use parametric adaptation [5].

An increase in reliability can be achieved by using interference-resistant codes, for example: LDPC codes [6, 7], turbo codes (TC) [8]. TC and LDPC codes are adopted by the fifth generation mobile communication standards 4G LTE and 5G, respectively.

4G and 5G systems use adaptive modulation, power, and coding techniques. In the article we will consider only the adaptation of coding. In 4G, 5G systems, during adaptation, the coding rate  $R$  is adjusted in the range from  $1/5$  to  $2/3$ . At the same time, the use of TC is more expedient at low coding rates, and LDPC codes - at high ones.

In 4G LTE, for high-speed transmission, TCs are used in combination with PSK-4, QAM-16, QAM-64 modulations, and for low-speed transmission, convolutional and block codes are used. In 5G systems, LDPC code is used for high speeds, polar codes are used for low speeds. How modulations are used PSK-4, QAM-16, QAM-64, QAM-256.

The high efficiency of turbo codes is due to the iterative decoding algorithms developed for them. Decoding algorithms developed for turbo codes use «soft» solutions at the input and output of the decoder. In this connection, they received the name of algorithms with «soft» input – «soft» output SISO (soft input - soft output). These algorithms include the Viterbi algorithm with a «soft» output SOVA (soft output Viterbi algorithm), the decoding algorithm based on the maximum a posteriori probability MAP (maximum a posteriori probabilities) or, as mentioned in some sources, the BCJR algorithm (Bahl-Cocke-Jelinek-Raviv), as well as less complex Max Log MAP and Log MAP algorithms [9].

According to the 3rd Generation Partnership Project (3GPP) TS 38.212, LDPC is recommended for the Fifth-generation (5G) New Radio (NR) shared channels due to its high throughput, low latency, low decoding complexity and rate compatibility. For LDPC codes, algorithms based on calculating the logarithmic ratios of the likelihood functions are also used: Sum Product Algorithm (SPA), Min-Sum Algorithm (MSA), Layered Sum Product Algorithm (LSPA), Layered Min-Sum Algorithm (LMSA), Layered Offset Min-Sum Algorithm (LOMSA).

## 2. Analysis of research and publications

In [10], a method is presented that solves two problems, namely, estimates of the logarithmic ratio of the likelihood function and quantization. This method is focused on high-performance computing units with low latency, achieved using deep neural networks.

The paper [11] presents the development of a turbo receiver based on the Bilinear Generalized Approximate Message Transfer (BiG-AMP) algorithm. In this turbo receiver, all received symbols are used to estimate the channel state, user activity, and program data symbols, which effectively exploit the common sparsity pattern. The extrinsic information from the channel decoder is used for joint channel estimation and data discovery.

In [12] proposes the use of a compression sounding (CS) channel estimator in a system using orthogonal frequency division multiplexing (OFDM) and software defined radio (SDR) devices. The application of compression sounding theory is enabled by using sparse reconstruction algorithms such as orthogonal match search (OMP) and compression sample match search (CoSaMP) to take advantage of the sparse nature of the pilot subcarriers used in OFDM, optimizing system throughput.

Paper [13] proposes a new method for iterative channel estimation and data decoding. In the proposed method, the probability of occurrence of transmitted symbols is shifted. The a priori information about the offset is used for the initial channel estimation. The proposed scheme is based on the parallel concatenation of two shifted convolutional codes, which are constructed as systematic recursive convolutional codes with state-dependent puncturing.

Paper [14] presents an iterative receiver for a channel with phase-coherent block fading. The receiver jointly estimates the channel and decodes a low density parity check (LDPC) code using a sum product algorithm.

### 3. Formulation of the problem

The purpose of the article is to develop an adaptive method for assessing the reliability of information under conditions of uncertainty through the use of a priori and a posteriori information of the decoder. The method makes it possible to adapt to changing the parameters of the encoder and decoder of the turbo code (LDPC code) by using the logarithmic ratios of the likelihood functions (LLRs) and the calculated values of the noise dispersion.

### 4. Presentation of the main material

3GPP TS 38.212 [15] standard defines the LDPC channel coding chain before the encoded information bits transmitted through the channel model. Figure 1 shows the LDPC encoding chain, which includes transport block CRC attachment, LDPC base graph selection, code block segmentation and code block CRC attachment, LDPC encoding, rate matching and code block concatenation. The LDPC channel coding chain after the encoded information bits transmitted through the channel model is known as LDPC decoding chain shown in Figure 2. The LDPC decoding chain is the reverse process of LDPC encoding chain.

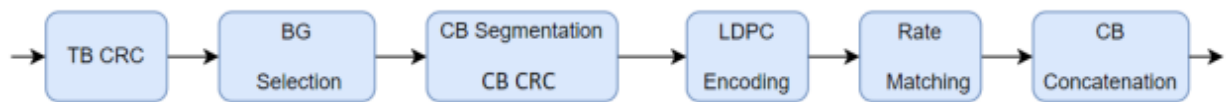


Figure 1: LDPC encoding

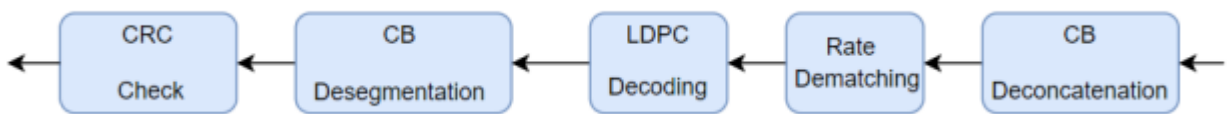


Figure 2: LDPC decoding

CRC is an error detection code used to measure BER after decoding. The entire transport block is used to calculate CRC parity bits.

**LDPC Encoding.** LDPC Encoding aims to add redundant bits to the message from the sender to get codeword which will be transmitted to the receiver. Assume the message to be encoded is denoted by  $m_1, m_2, m_3, \dots, m_K$ , where  $K$  is the number of message bits. The redundant bits are called parity bits denoted by  $p_1, p_2, p_3, \dots, p_L$ , where  $L$  is the number of the parity bits. The encoded message is called codeword denoted by  $c_1, c_2, c_3, \dots, c_N$ , where  $N$  is the number of encoded message bits. The procedure is shown in Figure 3.

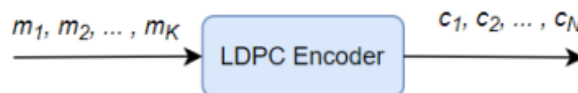


Figure 3: LDPC encoder

The message bits vector  $m$ , parity bits vector  $p$  and codeword bits vector  $c$  follow equation (1) and (2).

$$c^T = \begin{bmatrix} m^T \\ p^T \end{bmatrix} \quad (1)$$

$$H \times c^T = \mathbf{0} \quad (2)$$

Where  $\mathbf{H}$  is parity-check matrix,  $\mathbf{0}$  is  $N \times 1$  zero vector.

LDPC decoding. LDPC decoding tries to correct errors using message iterative algorithms. There are two kinds of decoding algorithms for LDPC decoding. One decoding algorithm is called hard decision decoding, in which the message passed contains the actual value of bits, such as Bit Flipping Algorithm. The other decoding algorithm is called soft decision decoding, in which the message passed is the probability value associated with the occurrence of a particular bit. We consider soft decision decoding algorithms because soft decision decoding algorithms in the log domain provide better performance than hard decision decoding algorithms.

LDPC codes can be represented using either parity matrix  $\mathbf{H}$  or Tanner graph introduced by Tanner [16]. There are two sections in the Tanner graph: variable nodes and check nodes corresponding to rows and columns in the parity-check matrix. An example is shown in Figure 4.

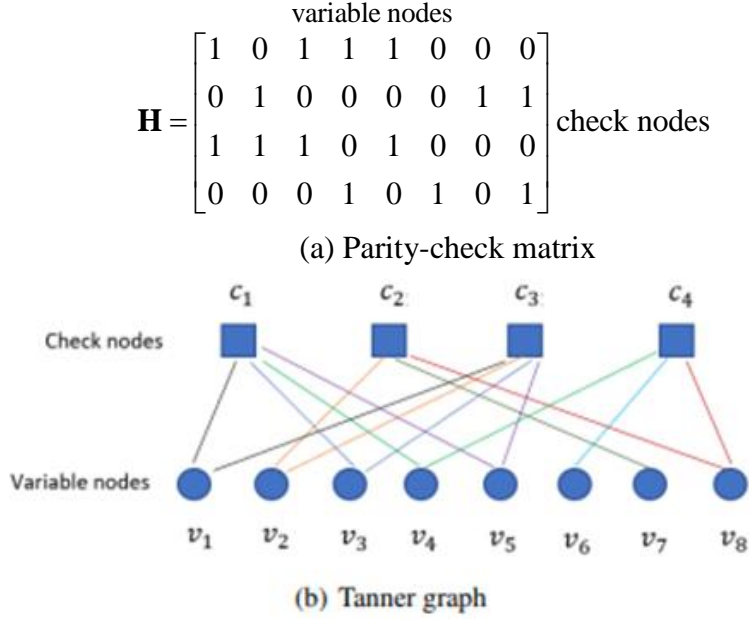


**Figure 4:** Parity-check matrix and Tanner graph

The input to LDPC decoder using log-likelihood ratios (LLR) value:

$$L(c_i) = \log \frac{P_r(c_i = 0 | y_i)}{P_r(c_i = 1 | y_i)} = \log \frac{P_r(x_i = +1 | y_i)}{P_r(x_i = -1 | y_i)}, \quad (3)$$

where  $L(c_i)$  is the input LLR to the decoder.

The variable nodes operation is shown in equation (4):

$$L(r_{ji}) = \log \frac{r_{ji}(0)}{r_{ji}(1)} = 2 \tanh^{-1} \left( \prod_{i' \in V_j/i} \tanh \left( \frac{1}{2} L(q_{i'j}) \right) \right) = \left( \prod_{i' \in V_j/i} a_{ij} \right) \varphi(\beta_{i'j}), \quad (4)$$

$$\text{where } r_{ji}(0) = \frac{1}{2} + \frac{1}{2} \prod_{i' \in V_j/i} (1 - 2q_{i'j}(1))$$

$$r_{ji}(1) = \frac{1}{2} - \frac{1}{2} \prod_{i' \in V_j/i} (1 - 2q_{i'j}(1))$$

$$q_{ij}(0) = (1 - P_i) \prod_{j' \in C_i/j} r_{ji}(0)$$

$$q_{ij}(1) = P_i \prod_{j' \in C_i/j} r_{j'i}(0)$$

$$\alpha_{ij} \equiv \text{sign}(L(q_{i'j}))$$

$$\beta_{i'j} \equiv |L(q_{i'j})|$$

$$\varphi(x) \equiv \log \frac{e^x + 1}{e^x - 1}$$

and  $q_{ij}(b)$  is the probability that  $c_i = b$ ,  $b \in \{0,1\}$ , given extrinsic information from all check nodes, excluding check node  $c_j$  and channel sample  $y_i$ ;  $r_{ji}(b)$  is the probability of the  $j^{\text{th}}$  check equation being satisfied given  $c^i = b$  and the other bits have separable distribution given by  $\{q_{ij'}\}_{j' \neq j}$ . Where  $V_j = \{\text{variable nodes connected to check node } j\}$ ,  $V_j/i = \{\text{variable nodes connected to check node } j\} / \{\text{variable node } i\}$   $C_i = \{\text{check nodes connected to variable node } i\}$   $C_i/j = \{\text{check nodes connected to variable node } i\} / \{\text{check node } j\}$   $P_i = P_r(c_i = 1/y_i)$ ,  $y_i$  is the channel sample at variable node  $i$ .

The check nodes operation is shown in equation:

$$L(q_{ij}) = L(c_i) + \sum_{j' \in C_i/j} L(r_{j'i})$$

$$L(Q_i) = L(c_i) + \sum_{j' \in C_i} L(r_{j'i})$$

Where  $L(Q_i)$  is the output LLR from the decoder and can be used to make decision.

On fig. 5 shows a block diagram of a two-component TC encoder.

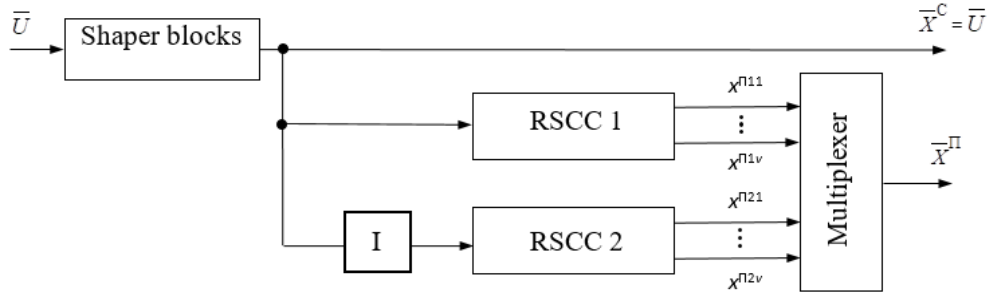


**Figure 5:** Structural diagram of the encoder TC

The TC encoder consists of a cascaded construction of recursive systematic convolutional codes (RSCC) connected in parallel, separated by an interleaver (I).

In fig. 6 shows the structural diagram of the multi-component TC encoder.

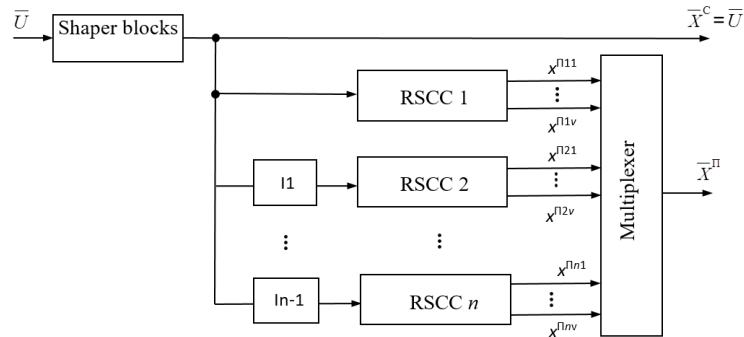


**Figure 6:** Structural diagram of the TC multi-component encoder

At the moment of time  $t$ , an information bit  $u_t$ ,  $t \in \overline{1, N}$  of a block of size  $N$ , is received at the RSCC input. The RSCC of the turbo code, depending on the value of the input bit, forms systematic  $c_t^C$  and

check bits  $c_t^{\text{II}}$ ,  $t \in \overline{1, N}$ ,  $c_t^{\text{C}}, c_t^{\text{II}} \in (0,1)$ . To implement the procedure of phase modulation of the PSK-2 signal, systematic  $c_t^{\text{C}}$  and check bits  $c_t^{\text{II}}$  are converted into systematic  $x_t^{\text{C}}$  and check symbols,  $x_t^{\text{II}}$ ,  $t \in \overline{1, N}$ ,  $x_t^{\text{C}}, x_t^{\text{II}} \in (-1,1)$ . The code word of the turbo code is formed by the parallel connection of two RSSCs separated by an interleaver. As a result of turbo coding, each systematic bit  $c_t^{\text{C}}$  will correspond to two check bits  $c_t^{\text{II1}}, c_t^{\text{II2}}$ , which are then converted into symbols  $x_t^{\text{C}}, x_t^{\text{II1}}, x_t^{\text{II2}} \in (-1,1)$ .

The effective representation of the "soft" solution or the logarithmic ratio of the likelihood functions (LLR) outside the decoder is defined by the expression [9]

$$L(x_t | y_t) = \ln \frac{P(y_t | x_t = +1)}{P(y_t | x_t = -1)} + \ln \frac{P(x_t = +1)}{P(x_t = -1)} = L_a(x_t) + L(y_t | x_t),$$

where  $L(y_t | x_t)$  is the LLR  $y_t$ , which is obtained by measuring  $y_t$  at the output of the channel during alternating conditions, which can be transmitted  $x_t = +1$  or  $x_t = -1$ , and  $L_a(x_t)$  is the a priori LLR of the data bit  $x_t$ . To simplify notation, equation (1) can be rewritten as follows[9]:

$$L'(x_t) = L_c(y_t) + L_a(x_t).$$

Here  $L_c(y_t)$  it means that the LLR member is obtained as a result of channel measurements made in the receiver. For systematic codes, the LLR at the output of the decoder is equal to the following [9]:

$$L(x_t) = L'(x_t) + L_e(x_t).$$

In this expression,  $L'(x_t)$  is the LLR outside the demodulator (at the decoder input), and  $L_e(x_t)$  is the «external» LLR, which represents external information resulting from the decoding process. From equations (2) and (3), the output LLR of the decoder will take the form:

$$L(x_t) = L_c(y_t) + L_a(x_t) + L_e(x_t).$$

The sign  $L(x_t)$  is a firm decision about the symbol  $x_t$ , and the modulus  $|L(x_t)|$  is the degree of reliability (plausibility) of this decision.

Decoder 1, in accordance with its algorithm, produces «soft» decisions about decoded symbols (output LLR), which consist of three parts [9]:

$$L^1(x_t^{\text{C}}) = L_c \cdot y_t^{\text{C1}} + L_a^1(x_t^{\text{C}}) + L_e^1(x_t^{\text{C}}),$$

where  $x_t^{\text{C}}$  is the systematic symbol of the TC encoder.

At the same time, the «external» information of decoder 1 about the symbol  $x_t^{\text{C}}$ , which is a priori for decoder 2 (taking into account the interleaving operation), will take the form [9]

$$L_e^1(x_t^{\text{C}}) = L_a^2(x_t^{\text{C}}) = L^1(x_t^{\text{C}}) - L_a^1(x_t^{\text{C}}) - L_c \cdot y_t^{\text{C1}}.$$

The second elementary decoder, having received a priori information about the information symbols, makes similar calculations, determining its «external» information about the symbol  $x_t^{\text{C}}$  [9]:

$$L_e^2(x_t^{\text{C}}) = L_a^1(x_t^{\text{C}}) = L^2(x_t^{\text{C}}) - L_a^2(x_t^{\text{C}}) - L_c \cdot y_t^{\text{C2}},$$

which enters the decoder 1 input of the next decoding iteration.

After performing the necessary number of iterations or in the case of a forced stop of the iterative decoding procedure, decisions are made about the decoded symbols:

$$x_t^{\text{C}} = \begin{cases} 1, & \text{if } L(x_t^{\text{C}}) \geq 0 \\ 0, & \text{if } L(x_t^{\text{C}}) < 0 \end{cases}.$$

As is known, the decoding of TC symbols takes place according to the diagram of the corresponding RSSC, while the transition recursion, direct recursion, reverse recursion, LLR at the output of the decoder and the parameter of «external» information are calculated [9]. Let's consider the features of calculating the output LLR for decoder 2, using the Map decoding algorithm.

The structural diagram of the three-component TC decoder model is shown in Fig. 7.

As in the case of two-component TC, three-component decoders work in series. A feature of the decoding of a three-component TC, in contrast to a two-component one, is that the a priori information for the component encoder is formed as the sum of not two, but three components: the channel reading of the systematic bit, as well as the values of the LLR obtained by the two previous component decoders (if necessary, with previous iteration, including interleaving (I)/deinterleaving (D) procedures).

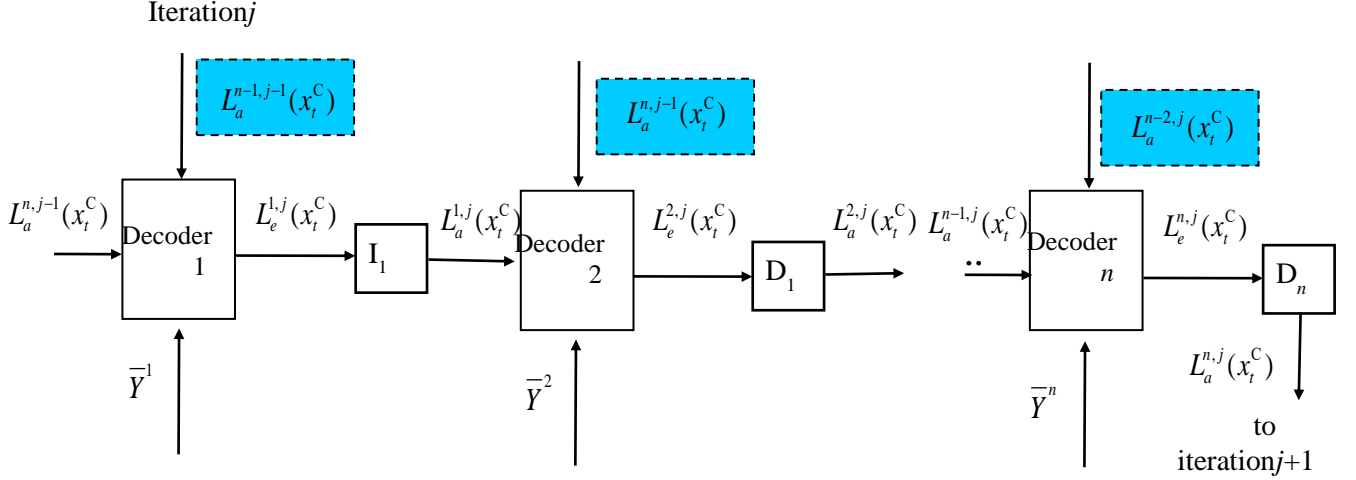


**Figure 7:** Structural diagram of a multi-component TC

The first decoder, using the "output" LLR, a priori LLR from the second and third decoders of the previous iteration and information from the channel, determines the "external" information about the symbol  $x_t^C$ :

$$L_e^{1,j}(x_t^C) = L^{1,j}(x_t^C) - L_a^{2,j-1}(x_t^C) - L_a^{3,j-1}(x_t^C) - L_c \cdot y_t^{C2}.$$

The second decoder uses the "source" LLR, the a priori LLR from the third decoder of the previous iteration and the a priori LLR from the first decoder of the current iteration, as well as information from the communication channel, to determine the "external" information about the symbol:

$$L_e^{2,j}(x_t^C) = L^{2,j}(x_t^C) - L_a^{3,j-1}(x_t^C) - L_a^{1,j}(x_t^C) - L_c \cdot y_t^{C2}.$$

The third elementary decoder, having received a priori information about the information symbols from the first and second decoders, as well as using the original LLR and the information received from the channel, determines its "external" information about the symbol  $x_t^C$ :

$$L_e^{3,j}(x_t^C) = L^{3,j}(x_t^C) - L_a^{2,j}(x_t^C) - L_a^{1,j}(x_t^C) - L_c \cdot y_t^{C2}.$$

There are three events about decision-making during decoding by the decoder  $d$ ,  $d \in \overline{1,2}$ , iterations of decoding  $j$ ,  $j \in \overline{1,I}$ , bits of information:

1) Event  $A_1$ .

Changed sign in values  $L_a^{d,j}(x_t^C)$  and  $L_e^{d,j}(x_t^C)$  iteration  $j$  does not occur ( $\text{sign}(L_a^{d,j}(x_t^C)) = \text{sign}(L_e^{d,j}(x_t^C))$ ),  $L(x_t^C) \geq 0$ . They will make a "firm" decision that the bit  $x_t^C = +1$  was passed.

2) Event  $A_2$ .

Changed sign in values  $L_a^{d,j}(x_t^C)$  and  $L_e^{d,j}(x_t^C)$  iteration  $j$  does not occur ( $\text{sign}(L_a^{d,j}(x_t^C)) = \text{sign}(L_e^{d,j}(x_t^C))$ ),  $L(x_t^C) < 0$ . They will make a "firm" decision that the bit  $x_t^C = -1$  was passed.

3) Event  $A_3$ .

The sign of the value of the a priori  $L_a^{d,j}(x_t^C)$  and the sign of the value of the a posteriori information  $L_e^{d,j}(x_t^C)$  of iterations  $j$  is not equal to zero ( $\text{sign}(L_a^{d,j}(x_t^C)) \neq \text{sign}(L_e^{d,j}(x_t^C))$ ). Decoding errors may occur.

The uncertainty index (error rate) for a two-component decoder  $d$ ,  $d \in \overline{1,2}$  decoding iteration  $j$ ,  $j \in \overline{1,I}$  is calculated using the following procedure:

$$\tilde{U}^{d,j} = \sum_{d=1}^2 R^{d,j}(t+1) = R^{d,j}(t) + 1, \text{if } \text{sign}(L_a^{d,j}(x_t^C)) \neq \text{sign}(L_e^{d,j}(x_t^C)), t \in \overline{1,N}.$$

In the case of applying adaptation and reconstruction of the decoder from two-component to multi-component, the uncertainty index for the decoder  $d$ ,  $d \in \overline{1,n}$ , decoding iteration  $j$ ,  $j \in \overline{1,I}$ , is calculated using the following procedure:

$$\tilde{U}^{n,j} = \sum_{d=1}^n R^{d,j}(t+1) = R^{d,j}(t) + 1, \text{if } \text{sign}(L_a^{d,j}(x_t^C)) \neq \text{sign}(L_e^{d,j}(x_t^C)), t \in \overline{1,N}.$$

The more often the values of the uncertainty index  $R$  increase, the more often incorrectly decoded bits appear, which leads to a deterioration in the reliability of information reception.

The total uncertainty index  $R_\Sigma$  is determined by the sum of the uncertainty indexes for all decoding iterations:

$$R_\Sigma = \sum_{j=1}^I R^{d,j}.$$

For the convenience of calculations and adaptation, we will normalize the uncertainty index:

$$\tilde{R}_\Sigma = \frac{R_\Sigma}{B \cdot \tilde{N} \cdot I} = \frac{\sum_{j=1}^I R^{d,j}}{B \cdot \tilde{N} \cdot I},$$

where  $B$  – is the number of data blocks of some observation window,  $\tilde{N}$  – is the variable size of the data block,  $I$  – is the number of turbo code decoding iterations.

When calculating the channel reliability parameter for the LLR, information about the value of the noise dispersion in the channel is used. We obtain analytical expressions for calculating the noise variance for a multicomponent decoder. This information will be used to improve the accuracy of calculating the decoding uncertainty index (error rate).

Let  $L_e$  – be a random variable, the values of which are the results of decoding by the  $i$ -th decoder, namely: calculation of LLR about transmitted bits in  $n$ -blocks of length  $N$ :  $L_e^i(x_{kt}^C)$ ,  $t \in \overline{1,N}$ ,  $k \in \overline{1,n}$ . The mathematical expectation and variance of the random variable  $L$  are defined by the following expressions:

$$M_{L_e} = \frac{\sum_{k=1}^n \sum_{t=1}^N L_e^i(x_{kt}^C)}{nN}, D_{L_e} = \frac{\sum_{k=1}^n \sum_{t=1}^N (L_e^i(x_{kt}^C) - M_{L_e})^2}{(n-1)(N-1)}.$$

In this case, with a two-component decoder, the interference variance for the  $n$ -th iteration of decoding of each channel of the OFDM system, taking into account the selected decoding algorithm, will be determined as follows (for the  $n$ -th iteration of decoding):

$$\hat{\sigma}_{n1}^2 = \frac{1}{N_1} \sum_{t=0}^{N_1-1} \left( (L^{1,n}(x_{1t}^C) + L^{2,n}(x_{1t}^C)) - \hat{y}_{1t} \right)^2, \dots, \hat{\sigma}_{nv}^2 = \frac{1}{N_v} \sum_{t=0}^{N_v-1} \left( (L^{1,n}(x_{vt}^C) + L^{2,n}(x_{vt}^C)) - \hat{y}_{vt} \right)^2.$$

With three-component decoding:

$$\hat{\sigma}_{n1}^2 = \frac{1}{N_1} \sum_{t=0}^{N_1-1} \left( (L^{1,n}(x_{1t}^C) + L^{2,n}(x_{1t}^C) + L^{3,n}(x_{1t}^C)) - \hat{y}_{1t} \right)^2, \dots,$$



$$\hat{\sigma}_{nv}^2 = \frac{1}{N_v} \sum_{t=0}^{N_v-1} \left( (L^{1,n}(x_{vt}^C) + L^{2,n}(x_{vt}^C) + L^{3,n}(x_{vt}^C)) - \hat{y}_{vt} \right)^2.$$

Accordingly, with four-component decoding:

$$\hat{\sigma}_{n1}^2 = \frac{1}{N_1} \sum_{t=0}^{N_1-1} \left( (L^{1,n}(x_{kt}^C) + L^{2,n}(x_{kt}^C) + L^{3,n}(x_{kt}^C) + L^{4,n}(x_{kt}^C)) - \hat{y}_{1t} \right)^2, \dots,$$

$$\hat{\sigma}_{nv}^2 = \frac{1}{N_v} \sum_{t=0}^{N_v-1} \left( (L^{1,n}(x_{kt}^C) + L^{2,n}(x_{kt}^C) + L^{3,n}(x_{kt}^C) + L^{4,n}(x_{kt}^C)) - \hat{y}_{vt} \right)^2,$$

where  $\hat{y}_{1t}$ ,  $\hat{y}_{vt}$  – are the estimated transmitted symbols for the 1st iteration of decoding the first and  $v$ -th channels, respectively;  $\hat{y}_{1t} = 1$ , if  $L_c \cdot y_{1t}^C > 0$  and  $\hat{y}_{1t} = -1$ , if  $L_c \cdot y_{1t}^C < 0$ , respectively  $\hat{y}_{vt} = 1$ , if  $L_c \cdot y_{vt}^C > 0$  and  $\hat{y}_{vt} = -1$ , if  $L_c \cdot y_{vt}^C < 0$ .

And so on, depending on the number of component encoders (decoders).

A block diagram of a two-component turbo code decoder with a decision block, which contains modules for calculating uncertainty indicators  $R^{d,j}$ ,  $R_\Sigma$ ,  $\tilde{R}$ , is shown in Fig. 8.

## 5. Analysis of the results

Simulation modeling was used to analyze the effectiveness of the method. For comparison, the fourth generation mobile communication standard LTE-Advanced was chosen. The simulation was carried out in the Visual Studio 2019 environment. A data transmission system was simulated with turbo codes, an OFDM modulator (demodulator), a channel with additive white Gaussian noise, modules for calculating the decoding error probability (the transmitted sequence was compared with the transmitted one - imitation of the service channel through which test information is transmitted to assess the reliability of information) and the indicator of decoding uncertainty (error rate). The values of the decoding uncertainty index (error rate) were calculated only on the basis of the decoding results. The simulation results were obtained based on the reliability  $\alpha = 0,95$ ,  $t_\alpha = 0,95$  (Laplace function argument), relative accuracy  $d = 0.1$ .

Turbo code was used with generators (1, 23/21), Log Map decoding algorithm, redundancy  $R = 1/3$ , pseudo-random and regular interleaver (de-interleaver), number of bits in the block  $N = 400$ , 1000. The signal-to-noise ratio changed from 0 up to 1.6 dB.

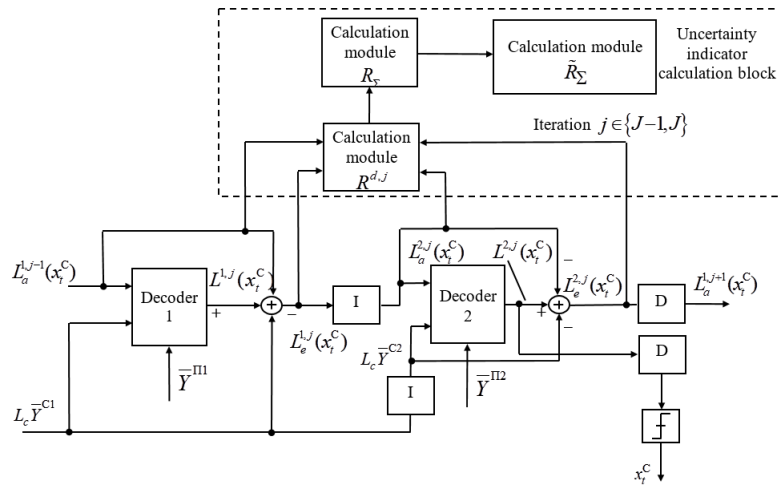


**Figure 8:** Block diagram of a TC decoder with a decoding uncertainty evaluation module

In fig. 9 shows the graphs of the dependence of the probability of a bit error  $P_{B \text{ dec}}$  and the uncertainty index (error coefficient) on the signal-to-noise ratio  $E_b / N_J$ , calculated by the standard method of simulation modeling, using the proposed method at 8 iterations of turbocode decoding, compared to the known approximate calculation method.

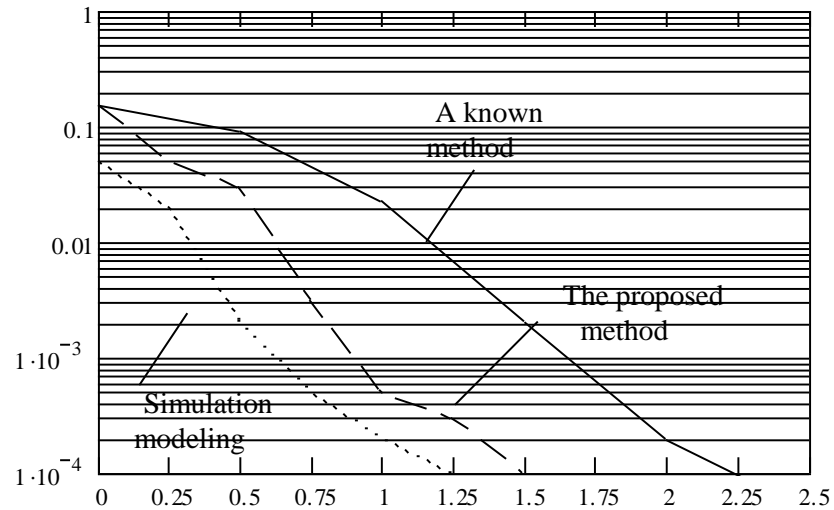


**Figure 9:** Graph of the dependence of the average probability of a bit error and the decoding uncertainty index (error rate) on the signal-to-noise ratio in the channel

The analysis shows that the proposed method provides greater accuracy in assessing the reliability of information in comparison with the closest analogue.

On fig. 10,11 shows graphical dependences of the average probability of a decoding bit error  $P_{B \text{ dec}}$  and the decoding uncertainty index (error rate) on the signal-to-noise ratio  $E_b / N_J$ , where  $E_b$  is the bit energy and  $N_J = \sigma^2 / 2$  is the spectral density.

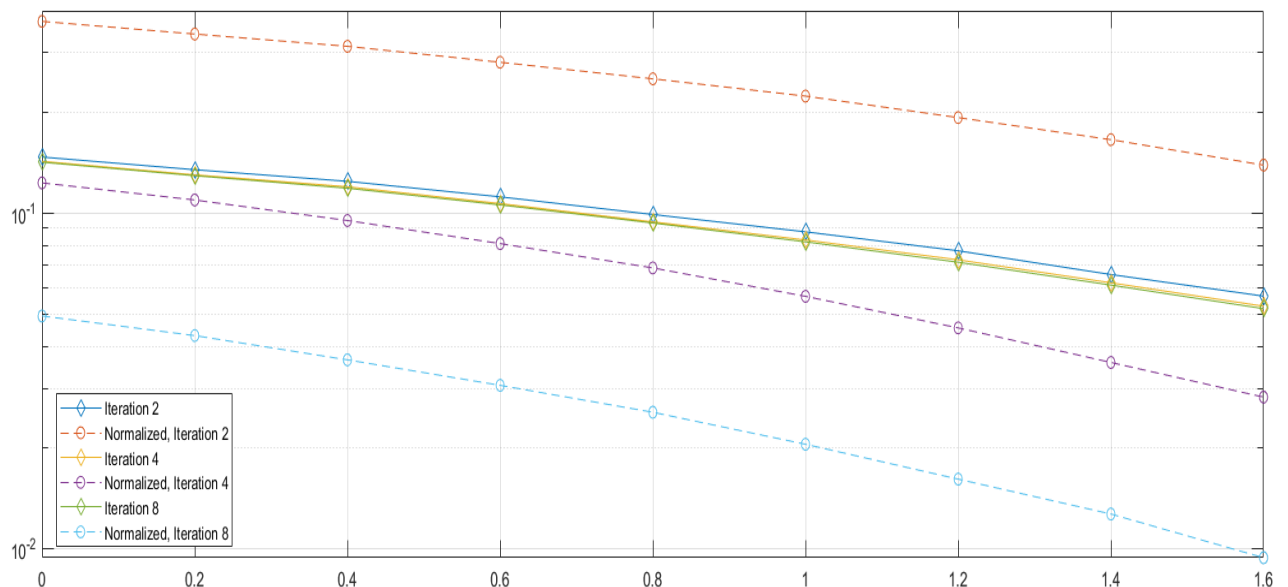


**Figure 10:** Graph of the dependence of the average probability of a bit error and the decoding uncertainty index (error rate) on the signal-to-noise ratio in the channel for  $N = 400$  and various decoding iterations

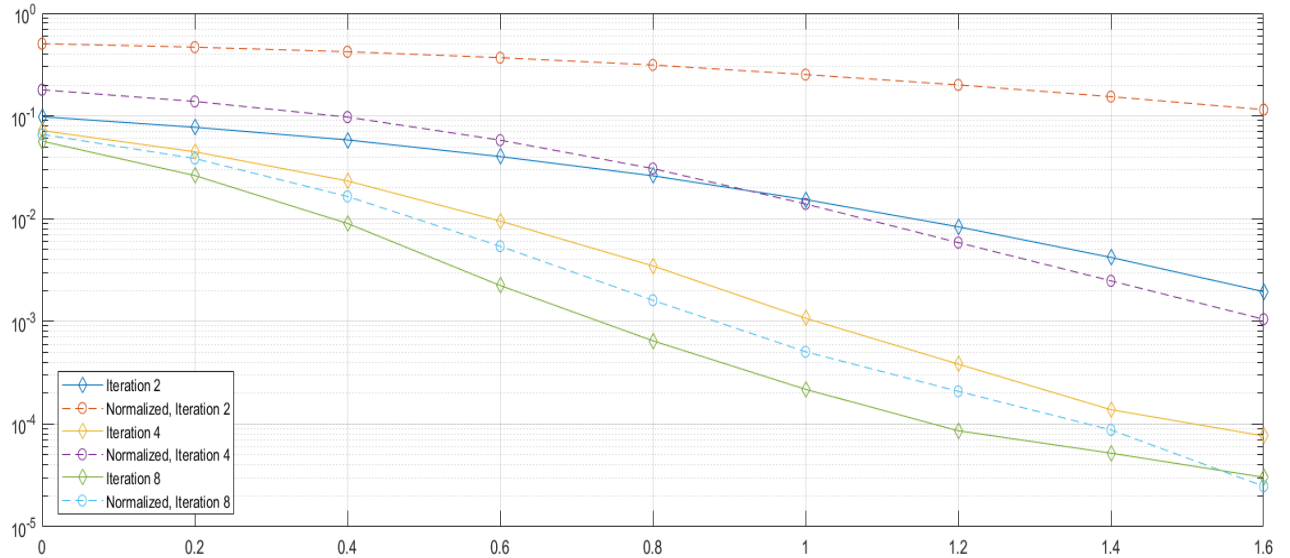


**Figure 11:** Graph of the dependence of the average probability of a bit error and the decoding uncertainty index (error rate) on the signal-to-noise ratio in the channel for  $N = 1000$  and various decoding iterations

Analysis of the simulation results shown in fig. 10, 11 shows that as the data block size increases from  $N = 400$  to 1000, the decoding uncertainty index (error rate) curve approaches the decoding error probability curve. For example, for  $N = 1000$ , 8 decoding iterations with a signal-to-noise ratio of 1.4 dB, the value of the decoding error probability is  $5 \cdot 10^{-5}$ , and the value of the decoding uncertainty index (error rate) is  $9 \cdot 10^{-5}$ . For  $N = 1000$ , 4 decoding iterations with a signal-to-noise ratio of 1.4 dB, the value of the decoding error probability is  $1,5 \cdot 10^{-4}$ , and the value of the decoding uncertainty index (error rate) is  $2,5 \cdot 10^{-3}$ .

An analysis of these graphical dependencies shows that with an increase in decoding iterations, the accuracy of estimating the reliability of information increases (the decoding uncertainty (error rate) curves approach the decoding error probability modelling curves).

The degree of similarity between decoding uncertainty indicators and decoding results will be estimated using the correlation function. The following figure shows graphical dependences of the correlation coefficient on the signal-to-noise ratio in the channel for  $N = 1000$  and various decoding iterations.

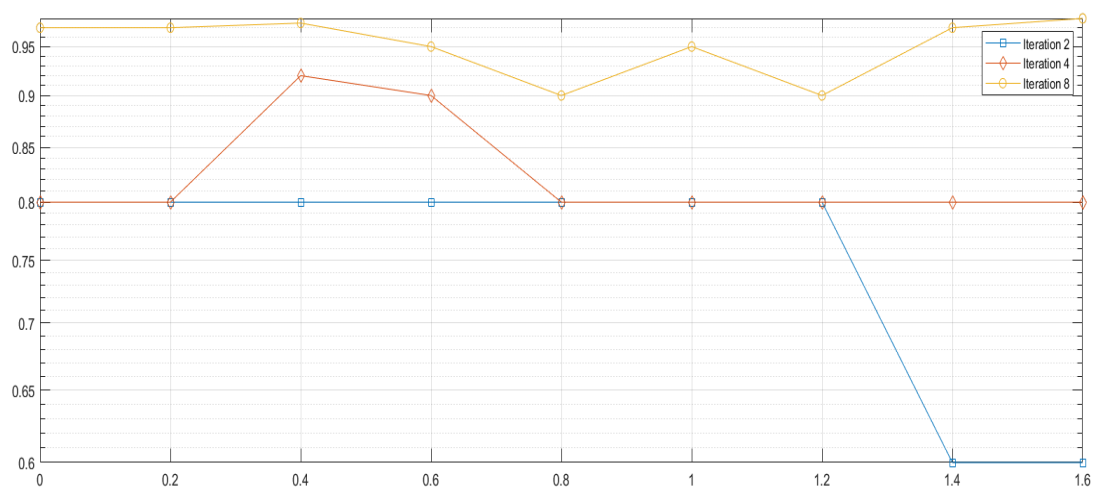


**Figure 12:** Graph of the dependence of the correlation coefficient on the signal-to-noise ratio in the channel for  $N = 1000$  and various decoding iterations

The analysis shows that with an increase in decoding iterations, the accuracy of assessing the

reliability of information increases, so for 8 decoding iterations, the values of the correlation coefficient change from 90 to 98%, for 4 iterations – from 80 to 92%, for 2 decoding iterations – from 60 to 80%.

## 6. Conclusion

1. The article proposes an adaptive method for assessing the reliability of information under conditions of uncertainty through the use of a priori and a posteriori information of the decoder. The method allows you to adapt to changing the parameters of the encoder and decoder of the turbo code (LDPC code) through the use of LRR and the calculated values of the noise dispersion.

2. In contrast to the known results, due to the use of the sign change of a priori and a posteriori LRR during iterative decoding and taking into account the noise dispersion values in the channel reliability parameter, the method allows obtaining information reliability values (error coefficient) without using an additional service channel.

3. Simulation analysis shows that with an increase in decoding iterations and the size of a data block, the accuracy of the information reliability estimate calculated by the decoder without reducing the throughput approaches the reliability estimate when using an additional service channel. So, for  $N = 1000$ , 8 decoding iterations with a signal-to-noise ratio of 1.4 dB, the value of the decoding error probability (when using an additional service channel) is  $5 \cdot 10^{-5}$ , and the value of the decoding uncertainty index (error rate) is  $9 \cdot 10^{-5}$ .

4. The method can be used in conjunction with other methods of parametric and structural adaptation under conditions of a priori uncertainty.

## 7. References

[1] Shafi M. 5G: A Tutorial Overview of Standards, Trials, Challenges, Deployment and Practice / Mansoor Shafi, Andreas F. Molisch, Peter J Smith, Thomas Haustein, Peiying Zhu, Prasan De Silva, Fredrik Tufvesson, Anass Benjebbour, Gerhard Wunder // IEEE Journal on Selected Areas in Communications.– 2017. – Vol. 35, no.6. – P. 1201-1221. DOI: 10.1109/JSAC.2017.2692307.

[2] Adebusola J.A. An Overview of 5G Technology / J. A. Adebusola, A. A. Ariyo, O. A. Elisha, A. M. Olubunmi, O. O. Julius // 2020 International Conference in Mathematics, Computer Engineering and Computer Science (ICMCECS). – 2020. – P. 1-4. DOI: 10.1109/ICMCECS47690.2020.240853.

[3] Globa L. Approach to building uniform information platform for the national automated ecological information and analytical system / L. Globa, S. Dovgiy, O. Kopiika, O. Kozlov // In: CEUR Workshop Proceedings, 3021. – 2021. – P. 53–65.

[4] Kopiika O. Use of service-oriented information technology to solve problems of sustainable environmental management / O. Kopiika, P. Skladannyi // In: CEUR Workshop Proceedings, 3021. – 2021. – P. 66–75.

[5] Zaitsev S. V. Structural adaptation of the turbo code coder and decoder for generating the transmission repeat request under conditions of uncertainty / S. V. Zaitsev, V. V. Kazymyr // Radioelectronics and Communications Systems. – Springer, 2017. – Vol. 60. – P. 18–27.

[6] Bae J. An overview of channel coding for 5G NR cellular communications / J. Bae & A. Abotabl, H. P. Lin, K. B. Song, J. Lee // APSIPA Transactions on Signal and Information Processing. – 2019. – P. 1-14. DOI: [10.1017/ATSIP.2019.10](https://doi.org/10.1017/ATSIP.2019.10).

[7] MacKay D. J. C. Near Shannon limit performance of low density parity check codes / D. J. C. MacKay, R. M. Neal // Electron. Lett. – 1996. – Vol. 32, no. 18. – P. 457–458.

[8] Arora K. A survey on channel coding techniques for 5G wireless networks / Arora K., Singh J., Randhawa Y.S. // Telecommun. Syst.– 2020. – Vol. 73 – P. 637–663.

[9] Berrou C. Codes and Turbo Codes / Berrou C. – Springer, 2010. – 415 p.

[10] Arvinte M. EQ-Net: Joint Deep Learning-Based Log-Likelihood Ratio Estimation and Quantization / Arvinte M., Tewfik A.H., Vishwanath S. // *ArXiv, abs/2012.12843v2*.

[11] Bian X. Joint Activity Detection and Data Decoding in Massive Random Access via a Turbo Receiver / X. Bian, Y. Mao, J. Zhang // 2021 IEEE 22nd International Workshop on Signal Processing Advances in Wireless Communications (SPAWC). – 2021. – P. 361-365. DOI: 10.1109/SPAWC51858.2021.9593149.

[12] Yanza-Verdugo A. Compressive Sensing Based Channel Estimator and LDPC Theory for OFDM using SDR / A. Yanza-Verdugo, C. Pucha-Cabrera, J. I. Ortega // Ingenius [online]. – 2020. – N.23. – P.74-85. <https://doi.org/10.17163/ings.n23.2020.07>.

[13] Takeuchi K. A Construction of Turbo-Like Codes for Iterative Channel Estimation Based on Probabilistic Bias / K. Takeuchi, R. R. Muller, M. Vehkaperä // 2011 IEEE Global Telecommunications Conference – GLOBECOM 2011. – 2011. P. 1-5. DOI: 10.1109/GLOCOM.2011.6133738.

[14] Jin X. Analysis of Joint Channel Estimation and LDPC Decoding on Block Fading Channels / Jin X., Eckford A. W., Fuja T. E. // International Symposium on Information Theory and its Applications, ISITA2004 Parma, Italy, October 10–13. – 2004. P. 679 – 684.

[15] «3GPP TS 38.212. Technical Specification Group Radio Access Network; NR; Multiplexing and channel coding (release 16)» [Online]. Available: <https://portal.3gpp.org/desktopmodules/Specifications/SpecificationDetails.aspx?specificationId=3214>

[16] Gallager R. Low-density parity-check codes / R. Gallager // IRE Transactions on Information Theory. – 1966. – Vol. 8, no. 1. – P. 21–28. DOI: 10.1109/TIT.1962.1057683